3-15-2016

The differential effects of low birth weight and Western diet consumption upon early life hepatic fibrosis development in guinea pig

Ousseynou Sarr
Western University

Alexandra Blake
Western University

Jennifer A. Thompson
Western University

Lin Zhao
Western University

Katherine Rabicki
Western University

See next page for additional authors

J Physiol 594.6 (2016) pp 1753–1772

The Journal of Physiology

The differential effects of low birth weight and Western diet consumption upon early life hepatic fibrosis development in guinea pig

Ousseynou Sarr[1,3,4], Alexandra Blake[2], Jennifer A. Thompson[2], Lin Zhao[1], Katherine Rabicki[2], Joanna C. Walsh[5], Ian Welch[6] and Timothy R. H. Regnault[1,2,3,4]

[1]*Department of Obstetrics and Gynecology, Western University, 1151 Richmond Street, London, ON, Canada, N6A 5C1*
[2]*Department of Physiology and Pharmacology, Western University, 1151 Richmond Street, London, ON, Canada, N6A 5C1*
[3]*Lawson Research Institute, 268 Grosvenor St, London, ON, Canada, N6A 4V2*
[4]*Children's Health Research Institute, 800 Commissioners Road East, London, ON, Canada, N6C 2V5*
[5]*Pathology and Laboratory Medicine, Western University, 1151 Richmond Street, London, ON, Canada, N6A 5C1*
[6]*Animal Care and Veterinary Services, Western University, 1151 Richmond Street, London, ON, Canada, N6A 5C1*

Key points

- Postnatal intake of a high saturated fat/high sugar diet, the Western diet (WD), is a risk factor for liver fibrosis. Recently, adverse *in utero* conditions resulting in low birth weight (LBW) have also been associated with postnatal fibrosis development.
- We demonstrate that suboptimal *in utero* conditions resulting in LBW are associated with changes in hepatic profibrotic genes in conjunction with minimal liver fibrosis in young non-overweight adult guinea pigs.
- Our results also indicate that WD promotes liver steatosis, enhanced expression of hepatic genes and proteins of the proinflammatory, profibrotic, cell death and collagen deposition pathways in conjunction with mild hepatic fibrosis.
- Our data highlight that pathways responsible for the initiation of a profibrotic state and ultimately hepatic fibrosis appear different depending upon the insult, an *in utero*-induced LBW outcome or a postnatal WD exposure.

Abstract Postnatal intake of an energy dense diet, the Western diet (WD), is a strong risk factor for liver fibrosis. Recently, adverse *in utero* conditions resulting in low birth weight (LBW) have also been associated with postnatal fibrosis development. We assessed the independent and possible synergistic effects of placental insufficiency-induced LBW and postnatal WD consumption on liver fibrosis in early adulthood, with a specific focus on changes in inflammation and apoptosis pathways in association with fibrogenesis. Male LBW (uterine artery ablation) and normal birth weight (NBW) guinea pig pups were fed either a control diet (CD) or WD from weaning to 150 days. Significant steatosis, mild lobular inflammation, apoptosis and mild stage 1 fibrosis (perisinusoidal or portal) were evident in WD-fed offspring (NBW/WD and LBW/WD). In LBW/CD *versus* NBW/CD offspring, increased transforming growth factor-beta 1 and matrix metallopeptidase mRNA and sma- and Mad-related protein 4 (SMAD4) were present in conjunction with minimal stage 1 portal fibrosis. Further, connective tissue growth factor mRNA was increased and miR-146a expression decreased in LBW offspring, irrespective of diet. Independent of birth weight, WD-fed offspring exhibited increased expression of fibrotic genes as well as elevated inflammatory and apoptotic markers. Moreover, the augmented expression of collagen, type III, alpha 1 and tumor necrosis factor-alpha was associated with increased recruitment of RNA polymerase II and enhanced histone acetylation (K9) to their respective promoters. These data support a role for both LBW and postnatal WD as factors contributing to hepatic fibrosis development in offspring through distinct pathways.

DOI: 10.1113/JP271777

(Resubmitted 23 October 2015; accepted after revision 6 December 2015; first published online 10 December 2015)
Corresponding author T. R. H. Regnault: Dental Science Building, Room 2021, Western University, 1151 Richmond Street, London, Ontario, Canada, N6A 5C1. Email: tim.regnault@uwo.ca

Abbreviations *ACTA2*, actin alpha 2 smooth muscle aorta; BAX, BCL2-associated X protein; BCL2, B-cell lymphoma 2; BCLXL, B-cell lymphoma-extra large; CD, control diet; ChIP, chromatin immunoprecipitation; *COL1A1*, collagen, type 1, alpha 1; *COL3A1*, collagen, type III, alpha 1; *CTGF*, connective tissue growth factor; ECM, extracellular matrix; HSC, hepatic stellate cell; IL1A, interleukin-1 alpha; *IL1B*, interleukin-1 beta; LBW, low birth weight; *MCP1*, monocyte chemotactic protein-1; miR, microRNA; *MMP2*, matrix metallopeptidase 2; NASH, non-alcoholic steatohepatitis; NBW, normal birth weight; SMAD4, Sma- and Mad-related protein 4; *TGFB1*, transforming growth factor-beta 1; *TIMP1*, tissue inhibitor of metalloproteinases-1; *TIMP2*, tissue inhibitor of metalloproteinases-2; *TNFA*, tumour necrosis factor-alpha; WD, Western diet.

Introduction

Liver fibrosis and its endstage, cirrhosis, represent the final common pathway of virtually all chronic liver diseases and remain major causes of morbidity and mortality worldwide (Iredale, 2007; Musso *et al.* 2010), where liver fibrosis is estimated to contribute to up to 45% of deaths in the developed world (Mehal *et al.* 2011). Liver fibrosis is also an important predictor of adverse long-term outcomes, including liver failure, diabetes and portal hypertension and is associated with an increased risk of liver cancer (Bhaskar, 2004; McCullough, 2004; Ekstedt *et al.* 2006).

Liver fibrosis is characterized by an excessive deposition and reorganization of extracellular matrix (ECM) with a dramatic increase in non-collagenous and collagenous ECM proteins, predominantly collagen I and collagen III (Iredale, 2007; Kwiecinski *et al.* 2011). Liver fibrosis as a later life cycle disease has been classically associated with chronic exposure to an unbalanced energy dense diet, such as a high/fat and high/sugar diet commonly termed a Western diet (WD), presenting itself in later age (Kohli *et al.* 2010; Ishimoto *et al.* 2013). In rodents chronically fed a WD diet enriched in saturated fats and cholesterol combined with fructose or sucrose in solid food or drinking water, a perisinusoidal fibrosis or a mild hepatic portal fibrosis in parallel with hepatic inflammation and overweight has been reported in adulthood (Panchal *et al.* 2012; Ishimoto *et al.* 2013; Longato, 2013). Moreover, male and female mice (weighing 25–30 g) consuming a 'Fast Food' diet that provides 40% of energy as fat (12% of saturated fat (by weight) and 2% of cholesterol (by weight)) supplemented with high-fructose corn syrup (42 g l^{-1} final concentration) in the drinking water for 25 weeks developed hepatic perisinusoidal and pericellular fibrosis (Charlton *et al.* 2011). These studies, while being valuable and demonstrating that the combination of saturated fats, fructose, sucrose and cholesterol in the WD is strongly associated with liver fibrosis development, have been mostly initiated in adolescent or mature subjects. While the links between childhood WD exposure and long-term hepatic fibrosis exist, to date the underlying transcriptional and epigenetic mechanisms remain unclear.

In addition to the classically held notion of the impact of a postnatal diet on the development of liver fibrosis, recent evidence suggests that the *in utero* environment may independently influence liver health. In young adult Danish LBW men, a strong and graded inverse relationship between small birth dimensions and mortality from cirrhosis, has been reported (Andersen & Osler, 2004). Further, liver fibrosis has been reported in a 3 month-old LBW infant suggesting the adverse intrauterine environment as a contributing factor for liver fibrosis development (Arai *et al.* 2010). These studies support the concept that the development of later life liver fibrosis may be set by factors associated with LBW. However, how pregnancy complications leading to LBW may independently promote fibrogenesis and fibrosis in adult life or influence postnatal diet-induced effects is ill defined.

Therefore, the aim of the present study was to evaluate the independent and possible synergistic roles of placental insufficiency-induced LBW and postnatal WD on the development of liver fibrosis in young growing animals through early adulthood. From a mechanistic perspective, we also compared changes in liver inflammatory, apoptotic and profibrotic pathways that have been implicated in the development of liver fibrosis in LBW, postnatal WD and LBW/postnatal WD situations.

Methods

Ethical approval

Animal care, maintenance, and surgeries were conducted in accordance with standards and policies of the Canadian Council on Animal Care, and the University of Western Ontario Animal Use Subcommittee reviewed and approved all procedures.

Animals and experimental design

Time-mated pregnant Dunkin-Hartley guinea pigs (Charles River Laboratories, Wilmington, MA, USA) were housed in a temperature (20 ± 2°C) and humidity (30–40%) controlled environment, with a 12 h light–dark cycle, and had access to guinea pig chow (LabDiet diet

5025: 27% protein, 13% fat and 60% carbohydrates as % of energy) and tap water *ad libitum*. All pregnant guinea pigs underwent uterine artery ablation at mid-gestation (~32 days, term ~69 days) to reduce placental blood flow and subsequently fetal growth as previously described (Turner & Trudinger, 2009; Sarr *et al.* 2014). Anaesthesia was induced using an anaesthetic chamber (4–5% isoflurane with 2 l min^{-1} O_2, followed by 2.5–3% isoflurane with 1 l min^{-1} O_2 for maintenance). Immediately after induction, a subcutaneous injection of Robinul (glycopyrrolate, 0.01 mg kg^{-1}; Sandoz Canada, Inc., Montreal, QC, Canada) was administered. Immediately following surgery, a subcutaneous injection of Temgesic (buprenorphine, 0.025 mg kg^{-1}; Schering-Plough Co., Kenilworth, NJ, USA) was administered, and monitoring of sows continued after surgery. Sows delivered spontaneously. At birth, all pups were weighed and at the end of pupping period, male guinea pigs pups were defined as normal birth weight (NBW) if their body weights were within the 25th and 75th percentile of all pups born, and LBW if their body weights were below the 25th percentile (Thompson *et al.* 2011). Based on this, NBW pups weights were greater than 90 g and LBW weights were below 85 g, similar to pup weight range allocations in uterine artery ligation and maternal feed restriction guinea pig models (Kind *et al.* 2003; Briscoe *et al.* 2004). From birth to weaning, pups were weighed daily. At 15 days of age, pups were weaned and housed in individual cages in a temperature (20 ± 2°C) and humidity (30–40%) controlled environment with a 12 h light–dark cycle. At this time, pups were randomly assigned either the control diet (CD; TD.110240; Harlan Laboratories, Madison, WI, USA) or the Western diet (WD; TD.110239; Harlan Laboratories) (Table 1) (Thompson *et al.* 2014). Animals were weighed twice weekly and feed intake monitored daily. At young adulthood, postnatal 150 days, (Gomez-Pinilla *et al.* 2007), animals were killed via CO_2 inhalation (Greulich *et al.* 2011) and the liver collected for histological, biochemical and molecular determinations. To avoid litter effects, only one LBW/NBW pup from a single litter was assigned to each diet.

Liver sampling

Immediately after the animal was killed, the thoracic cavity was opened and the whole liver removed and weighed. A representative 1 cm^2 central piece from the right lobe was placed directly in 4% paraformaldehyde for histology. The remaining right lobe was frozen in liquid nitrogen and stored at −80°C for later biochemical and molecular determinations.

Histopathological examination

Paraffin-embedded sections (5 μm) were stained with haematoxylin and eosin or Masson's trichrome for histological analysis of steatosis, inflammation and fibrosis. Stained slides were examined independently by veterinary and human pathologists (I.W. and J.C.W.). Steatosis was categorized as microvesicular or macrovesicular steatosis (Fiorentino *et al.* 2009).

Hepatic inflammation was graded as absent, minimal, mild, moderate and severe according to a procedure adapted from Knodell *et al.* (1981) and Ishak *et al.* (1995). 'Absent' reflected no inflammation. 'Minimal' inflammation denoted a few lobular or periportal inflammatory cells with no hepatocellular necrosis. 'Mild' inflammation represented lobular inflammation with occasional spotty liver cell necrosis ($\leq$1 focus per $\times$10 objective) or mild portal inflammation involving some or all portal areas. 'Moderate' inflammation corresponded to lobular inflammation with 2–4 foci of spotty necrosis per $\times$10 objective, zone 3 necrosis in some areas, and moderate portal inflammation involving some or all portal areas. 'Severe' inflammation, however, indicated lobular inflammation with $\geq$5 foci of spotty necrosis per $\times$10 objective, zone 3 necrosis and occasional portal–central bridging necrosis, and marked portal inflammation involving some or all portal areas.

Liver fibrosis was described as stages 0–4 based upon the fibrosis scoring system previously described by Kleiner *et al.* (2005) and used by Ishimoto *et al.* (2013): stage 0, no fibrosis; stage 1, perisinusoidal or portal fibrosis; stage 2, perisinusoidal and periportal; stage 3, bridging fibrosis; and stage 4, cirrhosis. Additionally, liver fibrosis was also quantitatively assessed using a computer-assisted morphometric analyser (Leica MM AF; Leica Microsystems CMS GmbH, Wetzlar, Germany) by analysing five random fields per slide and calculating the ratio of connective tissue to the whole liver slide area, expressed as fibrosis percentage.

TUNEL assay

TUNEL assay was employed to detect apoptotic cells using the In Situ Cell Death Detection Kit (Roche Applied Science, Indianapolis, IN, USA). In brief, the deparaffinized sections (5 μm) were incubated with 0.1% Triton X-100 solution–0.1% sodium citrate for 8 min at room temperature in order to permeabilize cell membranes. After two rinses in phosphate buffer solution (PBS), samples were incubated with the TUNEL reaction mixture that contains terminal deoxynucleotidyl transferase (TdT) and fluorescein-dUTP for 1 h at 37°C in a humidified chamber. After washing in PBS, slides were mounted with coverslips in 4′,6-diamidino-2-phenylindole (DAPI) mounting medium (Vector Laboratories, Burlingame, CA, USA) and sealed with nail polish. The DAPI and fluorescence-labelled images were visualized using a Leica Microscope (Leica Microsystems, Wetzlar, Germany).

Table 1. Composition of the experimental control diet (CD) and Western diet (WD)

Item	CD* (TD.110240)	WD* (TD.110239)
Main ingredients (g kg^{-1})		
Isolated soy protein	210	255
L-Methionine	2.47	3
Sucrose	100	190
Fructose	—	65
Corn starch	354	—
Maltodextrin	93	93
Cellulose	130	130
Soybean oil	60	—
Cocoa butter	—	50
Lard	—	55
Coconut oil	—	95
Cholesterol	—	2.5
Vitamin Mix Teklad (40060)	10	12.3
Vitamin C, L-ascorbyl-2-polyphosphate (35%)	0.61	0.75
Folic acid	0.008	0.01
Calcium phosphate dibasic	17.66	21.5
Potassium citrate, monohydrate	9.85	12
Magnesium oxide	2.63	3.2
Potassium chloride	3.29	4
Sodium chloride	1.64	2
Calcium carbonate	4.1	5
Ferric citrate	0.33	0.4
Manganese sulfate, monohydrate	0.164	0.2
Zinc carbonate	0.05	0.06
Cupric sulfate	0.0164	0.02
Potassium iodate	0.0008	0.001
Chromium potassium sulfate, dodecahydrate	0.008	0.01
Sodium selenite, pentahydrate	0.0008	0.001
Ammonium paramolybdate, tetrahydrate	0.0002	0.0003
Chemical composition		
Protein (% kcal)	21.6	21.4
Fat (% kcal)	18.4	45.3
Carbohydrates (% kcal)	60	33.3
Energy (kcal g^{-1})	3.4	4.2
Fatty acid composition (% of total fatty acids)		
Lauric acid (C12:0)	—	23.12
Myristic acid (C14:0)	—	8.83
Palmitic acid (C16:0)	11	17.32
Stearic acid (C18:0)	4	13.24
Oleic acid (C18:1*cis*9)	23.5	24.4
Linoleic acid (C18:2*n*−6)	53.4	4.2
α-Linoleic acid (C18:3*n*−3)	8	0.03

*Diets were formulated in the Harlan Laboratories (Madison, WI, USA).

DAPI and fluorescence-labelled images were merged and TUNEL-positive apoptotic cells in the merged images were quantified by the counting of positively stained cells. Three digital microscopic images at a magnification of ×100 were randomly captured at the areas where the positive cells were abundant for each section. The number of positively stained cells in the three images was averaged. The result was expressed as relative cell percentage per view field under the microscope.

Biochemical analysis

Hepatic lipids were extracted from 100 mg snap-frozen pieces of liver, using the method of Folch *et al.* (1957).

Quantification of hepatic lipids was determined as described previously (Assini *et al.* 2013). Briefly, [^{3}H]cholesteryl oleate (Amersham, GE Healthcare, Oakville, ON, Canada) was added to lipid extracts to assess recovery. A combined stock solution containing 200 μg ml^{-1} triolein and 200 μg ml^{-1} cholesterol was prepared in isopropanol and used to generate a standard curve ranging from 0.5 to 20 μg. Aliquots of standards and samples were dried under N_2 and 400 μl of chloroform added. Samples and standards were dried under N_2 and 500 μl of a 1% Triton X-100 solution in chloroform added. Following solublization, samples and standards were capped, left at room temperature for 1 h, and dried under N_2. A 50 μl volume of deionized water was added and incubated at 37°C for 15 min. Triglyceride, total cholesterol, and free cholesterol were then determined by enzymatic, colorimetric assays (triglyceride, Roche Diagnostics, Laval, QC, Canada; total cholesterol and free cholesterol, Wako, Richmond, VA, USA) according to manufacturer's instructions.

RNA preparation

Total RNA for mRNA and microRNAs (miRs) was isolated from snap-frozen ground liver (100 mg) using the TRIzol reagent (Invitrogen, Carlsbad, CA, USA) and the Purelink RNA Mini Kit according to manufacturer's instructions (Invitrogen, Burlington, ON, Canada). RNA yield was assessed by absorbance measurement at 260 nm on a Nanodrop 2000 (Thermo Fisher Scientific, Rochester, NY, USA) and integrity assessed on a denaturing 1.2% agarose gel stained with ethidium bromide.

Quantitative real-time reverse transcription polymerase chain reaction (RT-qPCR)

Liver mRNA and miR levels were determined by quantitative real-time PCR as follows: synthesis of cDNA was performed using 2 μg of RNA, random dodecamer primers and the M-MLV reverse transcriptase (Life Technologies, Burlington, ON, Canada). For miR analyses, 2 μg of RNA was reverse transcribed using the miScript II Reverse Transcription Kit according the manufacturer's instructions (Qiagen, Toronto, ON, Canada). EvaGreen technology coupled with designed primers (Table 2) and 3 μl of cDNA per reaction were used to quantify gene expression (Bio-Rad, Mississauga, Ontario, Canada). miR expression was quantified using 1 μl of cDNA and the miScript SYBR Green PCR Kit according manufacturer instructions (Qiagen). Standard curves for each primer pair were generated from serial dilutions of cDNA for determination of primer efficiencies. PCR efficiencies for each primer set were 90–100%. Melting curve analyses and the presence of a single amplicon at the expected size in 1.8% agarose gel confirmed amplification of a single product. Gene and miR targets were quantified using a Bio-Rad CFX384 RT-qPCR machine (Bio-Rad). mRNA expression was normalized to housekeeper GAPDH (Duan *et al.* 2014) and miR expression to miR-let-7a. There was no significant effect of either birth weight or diet on GAPDH mRNA or miR-let-7a expression. Control samples containing no cDNA were used to confirm the absence of DNA contamination. Each sample was run in triplicate. Expression of individual target genes or miRs was reported as fold changes relative to the control group using the $\Delta\Delta C_t$ method.

Chromatin immunoprecipitation

Chromatin immunoprecipitation (ChIP) was performed on snap frozen ground liver samples from offspring killed at 150 days of age. Snap frozen ground liver (50 mg) was homogenized and incubated in 1 ml of 1% formaldehyde for 30 min at room temperature to cross-link proteins and DNA. Glycine (1 M) was added to all samples to terminate cross-linking. All samples were centifuged at 2000 *g* at room temperature for 5 min and supernatants were subsequently removed. Each sample was then washed with PBS before being placed in 0.5 ml of SDS lysis buffer (1.1% SDS, 10 mM EDTA, 50 mM Tris HCl pH 8.0) with protease inhibitor cocktail (Roche, Mississauga, Ontario, Canada) and inverted during 20 min at 4°C. Lysates were diluted twofold with the addition of ChIP dilution buffer (1.1% Triton X-100, 1.2 mM EDTA, 167 mM NaCl and 16.7 mM Tris HCl pH 8.0). Samples were then sonicated for 4 × 30 s at 30 A on ice to produce sheared, soluble chromatin. Following a 16, 600 × g centrifugation for 10 min at 4°C, supernatants containing sheared chromatin were collected and the chromatin was quantified using BCA Protein Assay (Thermo Scientific, Waltham, MA, USA). The chromatin (500 μg from each sample) was incubated with 4 μg of antibodies against RNA polymerase II (cat. no. 05-623B, Millipore, Billerica, MA, USA) and histone H3 acetylated at lysine 9 (H3K9, cat. no. 06-942, Millipore) and rotated overnight at 4°C. For each sample, two corresponding aliquots were reserved as 'controls': one incubated without antibody ('input') and another with non-immune IgG (Millipore). Twenty-four hours later, protein A/G PLUS-Agarose beads (40 μl; Santa Cruz Biotechnology, Santa Cruz, CA, USA) was added to each tube, the mixtures rotated for 2 h at 4°C and the beads containing the immunoprecipitated complexes were collected by centrifugation at 106 × g for 2 min at 4°C. The beads/immunoprecipitated complexes were washed sequentially for 5 min in low salt wash buffer (20 mM Tris–HCl, pH 8, 2 mM EDTA, 0.1% SDS, 1% Triton X-100, 150 mM NaCl), high salt wash buffer (same as low salt wash buffer, except containing

Table 2. Primer sequences used to measure guinea pig hepatic mRNA and miR expressions by RTq-PCR

Gene/miR	Accession number*	Forward/reverse primer
TGFB1	NM_001173023.1	F: 5′-CAATTCCTGGCGCTACCTCA-3′
		R: 5′-ACCGATCCGTTGATTTCCA-3′
CTGF	XM_003468462.1	F: 5′-CACCCGGGTTACCAATGACA-3′
		R: 5′-CCGGTAGGTCTTCATGCTGG-3′
COL1A1	XM_003466865.1	F: 5′-AACGGAGACACCTGGAAACC-3′
		R: 5′-TTGACTAGGTCCAGGGCTGA-3′
COL3A1	XM_003478706.2	F: 5′-TGCTCGAAGTCCAGTTGG-3′
		R: 5′-ATTTGCACTGGCTGATCC-3′
ACTA2	ENSCPOT00000011693	F: 5′-GACATCAAGGAGAAGCTGTG-3′
		R: 5′-GCTGTTGTAGGTGGTTTCAT-3′
IL1B	NM_001172968.1	F: 5′-ACAATCTGAACCGACAAGTG-3′
		R: 5′-ACAGGCTTATGTTCTGCTTG-3′
MCP1	NM_001172926.1	F: 5′-GCTTGTGCTCCAACACTCCA-3′
		R: 5′-ACCCACTTCTGTGTGGGGTC-3′
TNFA	U77036	F: 5′-GCCGTCTCCTACCCGGAAAA-3′
		R: 5′-TAGATCTGCCCGGAATCGGC-3′
MMP2	XM_003477541.1	F: 5′-CAGGGCACCTCCTACAACAG-3′
		R: 5′-CCTTCTGAGTTCCCACCGAC-3′
TIMP1	XM_005000239.1	F: 5′-CAACGACATCCGGTTCCTCT-3′
		R: 5′-AAGTCTTGGTGACGCCCTTC-3′
TIMP2	NM_001173024.1	F: 5′-TGCACATCACCCTCTGTGAC-3′
		R: 5′-CAGCGCGTGATCTTGCATTC-3′
GAPDH	NM_001172951.1	F: 5′-GCTCGTTTCTTGGTATGACA-3′
		R: 5′-CTAGTCTCCATGGTCTCACT-3′
miR-378a	MS00013566	5′-CUCCUGACUCCAGGUCCUGUGU
miR-223	MS00033320	5′-UGUCAGUUUGUCAAAUACCCC
miR-let-7a	MS00033131	5′-UGAGGUAGUAGGUUGUAUAGUU
miR-27b	MS00000154	5′-UUCACAGUGGCUAAGUUCUGC
miR-29a	MS00033397	5′-UAGCACCAUCUGAAAUCGGUUA
miR-29c	MS00000175	5′-UAGCACCAUUUGAAAUCGGUUA
miR-146a	MS00000441	5′-UGAGAACUGAAUUCCAUGGGUU
miR-291b	MS00027223	5′-AAAGUGCAUCCAUUUUGUUAGU
miR-26a	MS00033348	5′-UUCAAGUAAUCCAGGAUAGGCU

*Accession number for sequences in the National Centre for Biotechnology Information (NCBI) database, Ensembl genome browser or Qiagen website. F: forward; R: reverse.

500 mM NaCl), LiCl wash buffer (10 mM Tris–HCl, pH 8, 1 mM EDTA, 1% NP-40, 1% deoxycholate, 0.25 M LiCl), and in 2 × TE buffer (20 mM Tris–HCl pH 8, 1 mM EDTA pH 8.0). The beads were then eluted with 250 μl elution buffer (10% SDS, 0.1 mM $NaHCO_3$ + 20 μg salmon sperm DNA) at room temperature. The elution step was repeated once and eluates were combined. Cross-linking of the immunoprecipitated chromatin complexes and 'input controls' was reversed by heating the samples at 65°C overnight. Proteinase K (3 μl of a 10 mg ml^{-1} stock (Invitrogen) diluted in 20 μl of 1 M Tris–HCl, pH 6.6 and 10 μl of 0.5 M EDTA) was added to each sample and incubated for 2 h at 45°C. The DNA was purified by phenol–chloroform extraction and precipitated in ethanol overnight at −20°C. The supernatant was removed and pellets were dried. Samples and 'input controls' were diluted in 50 μl of clean double distilled water. Real-time PCR was conducted using forward (5′-GGGTTACAAGGCGCAATAAA-3′) and reverse (5′-GAAAACAGCACATCTGGAAC-3′) primers (Life Technologies) that amplify a −206 bp to +71 bp region encompassing the TATA box and the COL3A1 (XM_003478706.2) initiation site. Forward (5′-CCCTCAGAGACTCCACTTTC-3′) and reverse (5′-GTTTGTTGGTTTGGGAGACC-3′) primers designed to amplify a −217 to −17 bp region encompassing the TATA box in the TNFA promoter (NM_001173025) were also employed. Recruitment of RNA polymerase II and acetylation of histone H3K9 in the promoter of *COL3A1* and *TNFA* genes were calculated by comparing the relative abundance of the immunoprecipitated chromatin compared with input chromatin using the $\Delta\Delta C_t$ method.

Table 3. Characteristics of guinea pigs given *ad libitum* CD or WD from weaning to 150 days

	CD		WD		Two-way ANOVA		
	NBW	LBW	NBW	LBW	BW	*d*	BW × *d*
Body weight (g)	758.0 ± 23.0	748.0 ± 33.0	739.0 ± 26.0	669.0 ± 22.0	0.16	0.089	0.28
Daily energy intake relative to body weight (kcal day^{-1} (g body weight)$^{-1}$)	59.88 ± 2.67	66.24 ± 5.16	69.79 ± 1.71	75.29 ± 8.37	0.20	<0.05	0.92
Relative liver weight (g (g body weight)$^{-1}$)	0.037 ± 0.003	0.037 ± 0.003	0.050 ± 0.003	0.051 ± 0.003	0.96	<0.001	0.92
Hepatic triglycerides (mg (g liver)$^{-1}$)	3.92 ± 0.74	5.51 ± 1.08	68.40 ± 11.39	75.74 ± 14.19	0.64	<0.001	0.76
Hepatic total cholesterol (mg (g liver)$^{-1}$)	2.72 ± 0.12	4.31 ± 0.35†	25.99 ± 3.5	21.30 ± 3.3	0.47	<0.001	0.15
Hepatic free cholesterol (mg (g liver)$^{-1}$)	2.34 ± 0.11	3.17 ± 0.21†	6.37 ± 0.42	6.09 ± 0.39	0.33	<0.001	0.06

Data are means ± SEM. *d*, diet; BW, birth weight. Two-way ANOVA and a Bonferroni *post hoc* test were used with birth weight (BW), diet (d) and their interaction (BW × d) as sources of variation. $^{\dagger}P < 0.01$ when comparing NBW/CD *versus* LBW/CD (n = 5–9 in each group).

Western immunoblotting

Proteins were extracted from homogenized snap-frozen ground liver (50 mg) in radioimmunoprecipitation assay (RIPA) buffer containing protease inhibitor cocktail (Millipore) and phosphatase inhibitors (1 M NaF, 0.2 M Na_2VO_4). Protein quantification was performed using a Pierce BCA Protein Assay (Thermo Scientific). The samples were separated on 8% SDS-PAGE and transferred onto Immobilon transfer membranes (Millipore). Non-specific protein binding was reduced by treating the membranes overnight with blocking buffer (5% milk, 10 mM Tris, 150 mM NaCl and 0.1% Tween). Blots were incubated with primary antibodies (caspase-3 (8G10), caspase-7 (D2Q3L), B-cell lymphoma 2 (BCL2)-associated X protein (BAX; sc-493), B-cell lymphoma-extra large (BCLXL; sc-7195) and interleukin-1 α (IL1A; D2Q3L), final dilution 1:1000) (Santa Cruz Biotechnology; Cell Signaling Technology, Inc., Danvers, MA, USA) at room temperature for 2 h. Mothers against decapentaplegic homolog 4 (SMAD4; cat. no. 9515, Cell Signaling Technology) and β-actin (A 5316, Sigma-Aldrich) antibodies were used at 1:2000 and 1:50,000 final dilutions for 3 h and 1 h, respectively, at room temperature. The donkey anti-rabbit (sc-2313) and anti-goat (sc-2020; horseradish peroxidase-conjugated secondary antibodies (1:5000 dilution; Cell Signaling Technology) were used for 1 h at room temperature. Protein bands were visualized by the Luminata Forte Western HRP Substrate (Millipore). The chemiluminescence signal was captured with a Luminescent Image Analyser (Bio-Rad), and densitometry values (arbitrary units) were determined using the ImageQuant LAS 4000 software (Bio-Rad). β-Actin protein was used as a loading control.

Statistical analysis

All data were statistically analysed by the GraphPad software (Prism 5.0; GraphPad, San Diego, CA, USA). Results were expressed as means ± SEM. A two-way ANOVA was performed to analyse the main effect and the interaction effect of birth weight and postnatal diet. A Bonferroni *post hoc* test was used to compare NBW/CD *versus* LBW/CD as well as NBW/WD *versus* LBW/WD. Comparisons between the two pup groups at birth were evaluated using an unpaired Student's *t* test. $P < 0.05$ was considered statistically significant.

Results

Body weights, food intake and intrahepatic lipids

While LBW male guinea pig pups (n = 12) were significantly lighter than the NBW male pups (n = 15) at birth (78.03 ± 1.87 *versus* 106.40 ± 2.74; $P < 0.0001$), at postnatal day 150, body weights were not increased in LBW/CD offspring or the WD-fed offspring, NBW/WD and LBW/WD (P = 0.13 and 0.08, respectively; Table 3). When adjusted for energy intake (daily energy intake divided by body weight), WD-fed offspring displayed higher calorie intake compared to CD-fed guinea pigs irrespective of birth weight (+15%, $P < 0.05$; Table 3). The liver weight to body weight ratio was 37% greater in WD-fed offspring (NBW/WD and LBW/WD) than in CD-fed offspring (NBW/CD and LBW/CD) independent of birth weight ($P < 0.001$; Table 3). Irrespective of birth weight, hepatic triglyceride, total cholesterol and free cholesterol levels were elevated in WD feeding (+1532%, +637% and +139%, respectively, $P < 0.001$; Table 3). Examination of LBW/CD offspring highlighted that total cholesterol and free cholesterol were increased when compared to NBW/CD offspring (+59% and +39%, respectively, $P < 0.01$; Table 3).

Hepatic steatosis, inflammation and fibrosis

The increased hepatic triglyceride accumulation in WD-fed offspring was associated with the development

of macro- and microvesicular steatosis (Fig. 1; Table 4). Moderate to severe macrovesicular steatosis was predominantly present in NBW/WD offspring, whereas most of LBW/WD offspring developed a mild to moderate microvesicular steatosis (Fig. 1*C* and *D*; Table 4). Minimal lobular inflammation (scattered inflammatory cells) was observed in LBW/CD relative to NBW/CD offspring (Fig. 2*A* and *B*; Table 4). In both NBW/WD and LBW/WD, a mild lobular inflammation was present (Fig. 2*C* and *D*; Table 4). Trichome stained liver sections from NBW/CD offspring livers displayed stage 0 fibrosis (Fig. 3*A*; Table 4). In the LBW/CD *versus* NBW/CD group, stage 1 portal fibrosis was observed but the mean percentage of collagen in the portal area was not statistically different (1.7 *versus* 3.6%, $P = 0.71$) (Figs 3*B* and 5*A*; Table 4). A significant collagen accumulation was observed in WD-fed animal with the NBW/WD displaying a stage 1 perisinusoidal fibrosis, whereas LBW/WD exhibited a stage 1 periportal fibrosis phenotype (Figs 3*C* and *D*, and 5*A*; Table 4).

LBW/CD and WD-fed offspring exhibited differential expression of inflammation and fibrosis markers at 150 days of age

Analysis of the genes involved in inflammation highlighted that WD-fed (NBW/WD and LBW/WD) offspring displayed higher *TNFA* (tumour necrosis factor-α), *IL1B* (interleukin-1 beta) and *MCP1* (monocyte chemotactic protein-1) mRNA expression (1.5-fold, $P < 0.05$; 1.8-fold, $P < 0.01$; 14.2-fold, $P < 0.01$; Fig. 4*A*) irrespective of birth weight. In addition, a significant increase in IL1A protein abundance was also observed in WD-fed offspring irrespective of birth weight (2.6-fold, $P < 0.001$; Fig. 4*B*). To investigate whether LBW or WD altered acetylated histone levels and RNA polymerase II recruitment at the

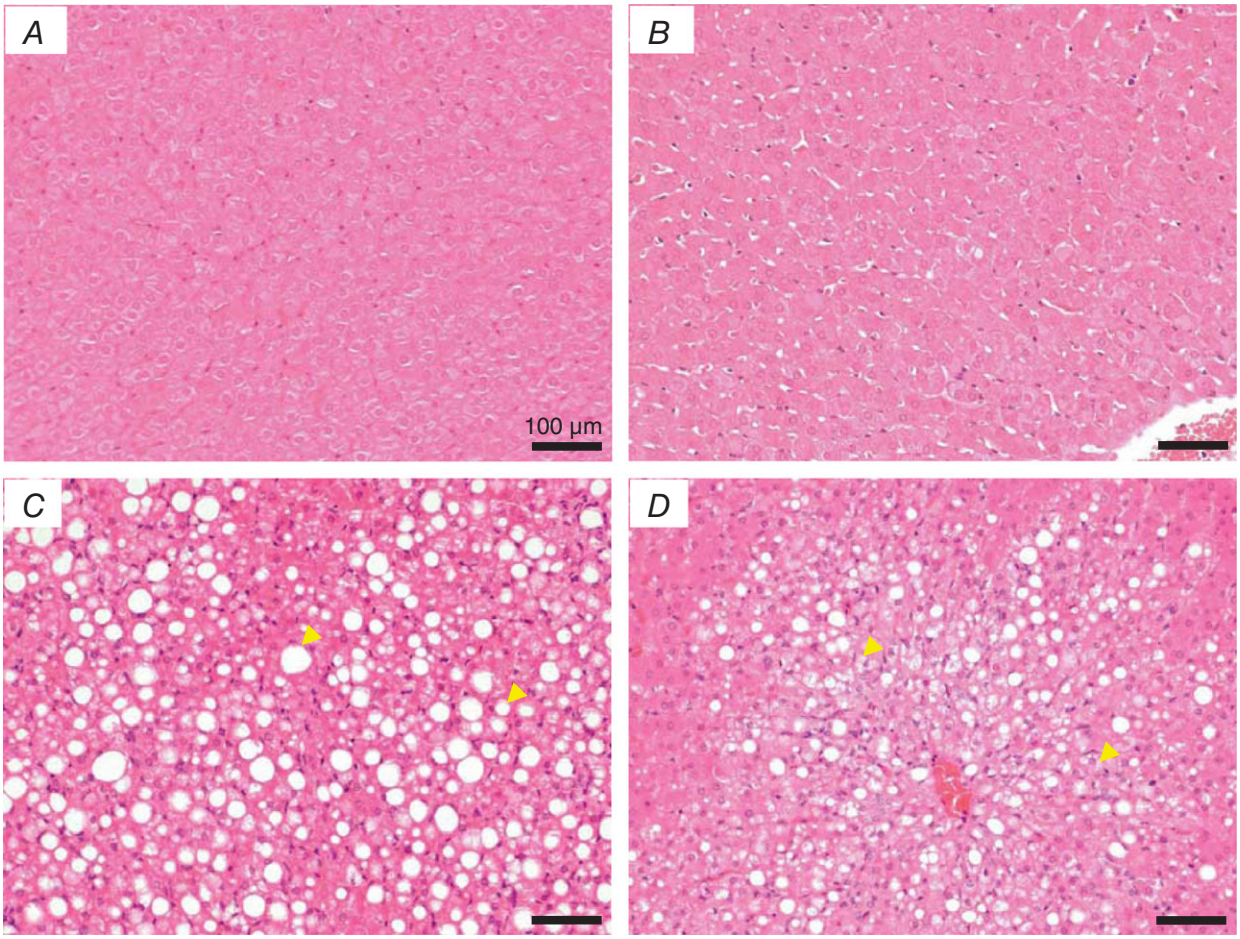

Figure 1. Intrahepatic lipid accumulation
NBW and LBW offspring were given *ad libitum* WD from weaning to 150 days. Representative images (×20 magnification) of haematoxylin and eosin-stained liver of NBW/CD (*A*), LBW/CD (*B*), NBW/WD (*C*) and LBW/WD (*D*) guinea pigs. Yellow arrowheads indicate lipid vesicles. Scale bar = 100 μm.

Table 4. Liver pathology of NBW and LBW guinea pigs fed *ad libitum* either the control (CD) or Western diet (WD) from weaning to 150 days

	CD		WD	
Birth phenotype	NBW	LBW	NBW	LBW
Steatosis				
None	5/5	4/4	0/5	0/5
Macrovesicular (exclusive or predominant)	0	0	4/5	1/5
Microvesicular (exclusive or predominant)	0	0	1/5	4/5
Portal inflammation				
None	5/5	3/4	5/5	4/5
Minimal	0/5	0/4	0/5	0/5
Mild	0/5	1/4	0/5	1/5
Moderate	0/5	0/4	0/5	0/5
Severe	0/5	0/4	0/5	0/5
Lobular inflammation				
None	4/5	0/4	1/5	1/5
Minimal	1/5	3/4	0/5	0/5
Mild	0/5	0/4	3/5	4/5
Moderate	0/5	0/4	1/5	0/5
Severe	0/5	0/4	0/5	0/5
Fibrosis				
None	5/5	0/4	0/5	0/5
Perisinusoidal or periportal	0/5	4/4	5/5	4/5
Perisinusoidal and portal/periportal	0/5	0/4	0/5	0/5
Bridging fibrosis	0/5	0/4	0/5	1/5
Cirrhosis	0/5	0/4	0/5	0/5

TNFA promoter, ChIP was performed. ChIP revealed that in the livers of WD-fed offspring, irrespective of birth weight, there was a significant increase in the recruitment of RNA polymerase II and in the acetylation of histone H3 (K9) in the proximal site of the *TNFA* promoter when compared to CD-fed offspring (1.5-fold, $P < 0.05$; Fig. 4*C* and *D*).

Despite a minimal portal fibrosis, LBW/CD offspring also displayed an increased expression of profibrotic- and ECM-related genes (Fig. 5*B*). Specifically, *TGFB1* (transforming growth factor-beta 1) and *MMP2* (matrix metallopeptidase 2) mRNA expression was increased in LBW/CD (3.4-fold, $P < 0.05$; 3.9-fold, $P < 0.01$, respectively; Fig. 5*B*). In addition, *CTGF* (connective tissue growth factor) mRNA expression was increased in LBW offspring irrespective of the diet consumed (1.8-fold, $P < 0.05$; Fig. 5*B*). Further, LBW/CD offspring displayed a higher increase in SMAD4 protein when compared to NBW/CD offspring (1.8-fold, $P < 0.05$; Fig. 5*C*). Corresponding to the observed phenotype, WD-fed offspring, irrespective of birth weight, showed increased *TGFB1, COL3A1* (collagen, type III, alpha 1), *COL1A1* (collagen, type 1, alpha 1), *TIMP1* and *TIMP2* (tissue inhibitor of metalloproteinases-1 and -2), *MMP2* and *ACTA2* (actin, alpha 2, smooth muscle, aorta) mRNA expression (1.8-fold, $P < 0.05$; 4.9-fold, $P < 0.01$; 3.2-fold, $P < 0.05$; 5.4-fold, $P < 0.001$; 3.7-fold, $P < 0.05$; 1.6-fold, $P < 0.057$, 3.1-fold, $P < 0.01$, respectively; Fig. 5*B*). For *COL1A1*, mRNA expression, birth weight and diet showed an interaction (BW × *d*) that indicated that the increase in *COL1A1* mRNA in LBW offspring on a WD was not as prominent as it is in NBW/WD offspring (Fig. 5*B*). Interestingly, birth weight or diet did not individually affect the acetylation of histone H3K9 in the *COL3A1* promoter (Fig. 5*D*). However, concomitant with the elevated *COL3A1* mRNA expression, RNA polymerase II recruitment at the *COL3A1* promoter region was increased in WD-fed offspring irrespective of birth weight (1.5-fold, $P < 0.05$; Fig. 5*E*).

LBW and WD differentially impact profibrotic-related miRNAs at 150 days of age

The expression of fibrosis-related miR species including miR-146a, miR-29c, miR-29a, miR-26a, miR-27b, miR-223 and miR-328 (Roderburg *et al.* 2011; He *et al.* 2012*a*,*b*) was analysed. While, miR-29a, miR-26a, miR-27b, miR-223 and miR-328 were not impacted by diet or birth weight ($P > 0.10$; Fig. 6), miR-146a expression was decreased in LBW, irrespective of diet (2.4-fold, $P < 0.01$), and miR-29c expression had a tendency to be reduced in WD-fed offspring independent of birth

weight (1.8-fold, $P = 0.067$; Fig. 6). Further, in LBW/WD relative to NBW/WD, the decrease in miR-146a was more pronounced (3-fold, $P < 0.01$).

WD feeding increased TUNEL-positive cells in conjunction with activated hepatic apoptosis pathway at 150 days of age

TUNEL staining of liver sections showed a 2.5-fold increase of positive cells in WD-fed offspring compared with CD-fed offspring irrespective of birth weight (Figs 7 and 8*C*). Correspondingly, WD induced a decrease in BCLXL protein abundance (1.3-fold, $P < 0.05$) while increasing procaspase-3, cleaved caspase-3, procaspase-7 and BAX protein abundances (1.5-fold, $P < 0.05$; 2.6-fold, $P < 0.001$; 1.5-fold, $P < 0.01$; 3.1-fold, $P < 0.001$, respectively; Fig. 8*A* and *B*). Procaspase-3, cleaved casapase-3, procaspase-7, BAX and BCLXL protein levels were not significantly impacted by birth weight ($P > 0.10$).

Discussion

This study identified changes in key hepatic profibrotic genes that appear to be maintained in young non-overweight adults following an adverse *in utero* environment leading to LBW. In these LBW offspring, raised on a CD, the expression of a number of hepatic profibrotic genes was significantly increased, in conjunction with a minimal portal fibrosis. Interestingly, the expression of these profibrotic genes was also increased in WD-fed non-overweight offspring who displayed a more severe hepatic fibrosis, though a number of profibrotic genes and proteins appeared to be WD specific and were not impacted by LBW alone (see summary in Fig. 9). Additionally, the lack of synergistic effects between LBW

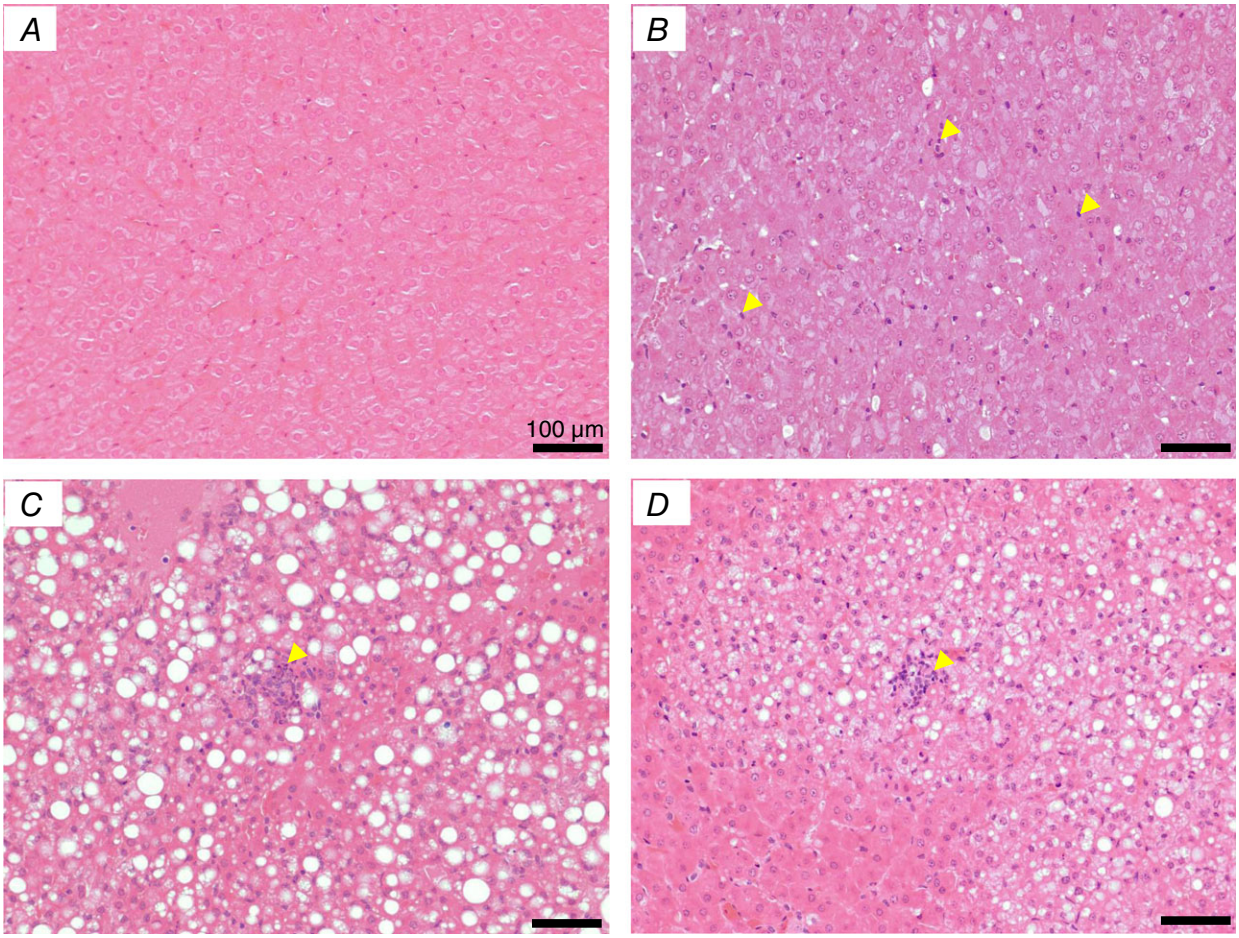

Figure 2. Inflammation in the liver of NBW and LBW guinea pigs with different dietary treatments
Representative histological inflammation changes in haematoxylin and eosin-stained liver (×20 magnification) of NBW/CD (*A*), LBW/CD (*B*), NBW/WD (*C*) and LBW/WD (*D*) offspring. Yellow arrowheads indicate inflammatory cells. Scale bar = 100 μm.

and WD at the age studied, together with the differential miR expression and apoptotic patterns, highlights differential pathways and developmental profiles for LBW and WD as to the initiation of a profibrotic state and ultimately hepatic fibrosis.

Features of metabolic syndrome classically associated with LBW/intrauterine growth restriction (IUGR) are insulin resistance, hypertension, dyslipidaemia, impaired glucose tolerance and type 2 diabetes. Very recently, fatty liver, non-alcoholic steatohepatitis (NASH), with or without fibrosis, has also been included among the persistent IUGR-dependent metabolic dysfunctions (Alisi *et al.* 2011). Indeed, Danish LBW men in early adult age (from age 15 to 49 years) displayed a strong and graded inverse association between small birth dimensions and mortality from cirrhosis, the more advanced form of liver fibrosis (Andersen & Osler, 2004). Further, in a single case report, liver fibrosis in a 3 month-old LBW infant has been characterized by both increased numbers of TGFB1- as well as ACTA2-positive hepatic cells (Arai *et al.* 2010). Although comparisons between different species should be interpreted carefully, in the current study it is interesting to note that in addition to a minimal collagen accumulation in young adult LBW offspring fed the CD, the steady-state mRNA expression of *TGFB1*, *CTGF* and *MMP2*, key profibrotic factors, was markedly increased.

TGFB1 mediates an enhanced expression of profibrogenic cytokine CTGF through SMAD phosphorylation and p38 MAP kinase activation, promoting liver fibrosis (Nagaraja *et al.* 2012). In addition, stimulation of hepatic stellate cells (HSCs) with TGFB1 production resulted in upregulation of MMP2 expression and activity (Yang *et al.* 2003), and, in severe hepatic fibrosis, MMP2 gene expression and activity are increased (Takahara *et al.* 1995), accelerating disease progression through degradation of normal liver matrix and pro-proliferative effects on HSCs (Benyon & Arthur, 2001). TGFB1 is becoming recognized as being central to sustained

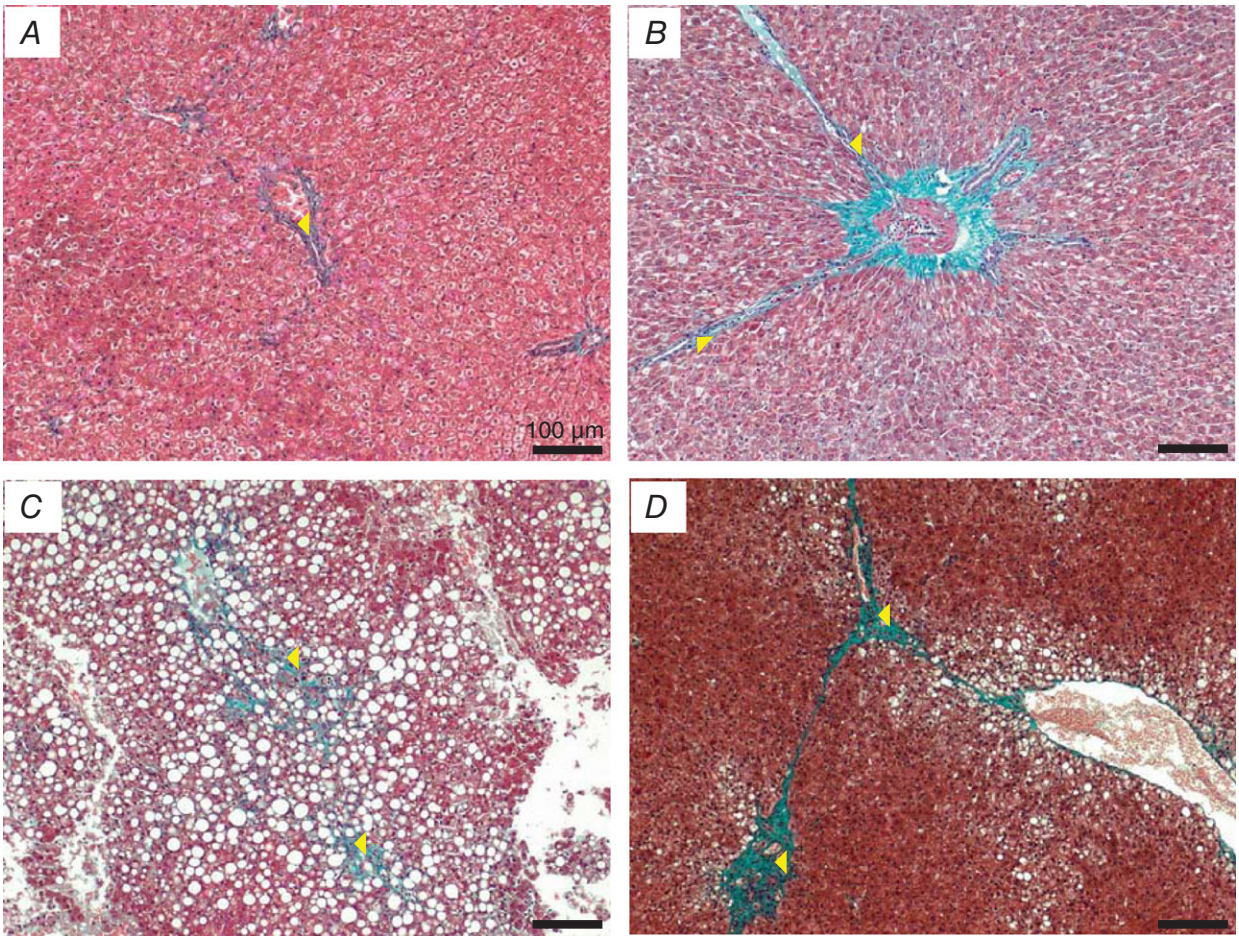

Figure 3. Hepatic fibrosis
Representative images (×10 magnification) of trichrome-stained liver of NBW/CD (*A*), LBW/CD (*B*), NBW/WD (*C*) and LBW/WD (*D*) offspring. The trichrome stain highlights 'chicken-wire' fibrosis/collagen in blue (yellow arrowheads). Scale bar = 100 μm.

upregulation of downstream genes involved in fibrotic development in various organs (Lan *et al.* 2011). Possible modulators of this sustained TGFB1 action include hypoxia and oxidative stress. Indeed, in carbon tetrachloride-induced cirrhosis, hypoxia promotes TGFB1 production in hepatocytes (Jeong *et al.* 2004) and in hypoxia-inducible factor 1-alpha knockdown studies, transcription of *IL6*, *TGFB* and *CTGF*, and secretion of collagen I are inhibited (Wang *et al.* 2013), demonstrating possible hypoxic regulation of inflammatory/TGFB activated fibrotic pathways. The situation of placental insufficiency, resulting in LBW, is an environment often characterized by hypoxia and oxidative stress (Hutter *et al.* 2010) as well as lack of nutrients for the fetus. Potentially, within this adverse *in utero* environment, fetal activated TGFB fibrotic pathways may be perceived as a pathological response to the *in utero* inadequate environment and this activated state may persist into postnatal life. Interestingly, the concept of a primed or sustained activation of TGFB fibrotic pathways has now been reported to occur in chemically induced fibrosis models in rats, viral hepatitis-induced fibrosis in patients and diet-induced fibrosis in rats (Matsuzaki *et al.* 2007; He *et al.* 2012*a*; Kim *et al.* 2014). Our study suggests that in the LBW situation, an activated profibrotic pathway, possibly through hypoxia and/or nutrient deficiency, could set the stage for a sustained activation of a fibrotic pathway into postnatal life. This highlights the critical role of a sub-optimal *in utero* environment in modulating a hepatic profibrotic gene signature in early adulthood, though the

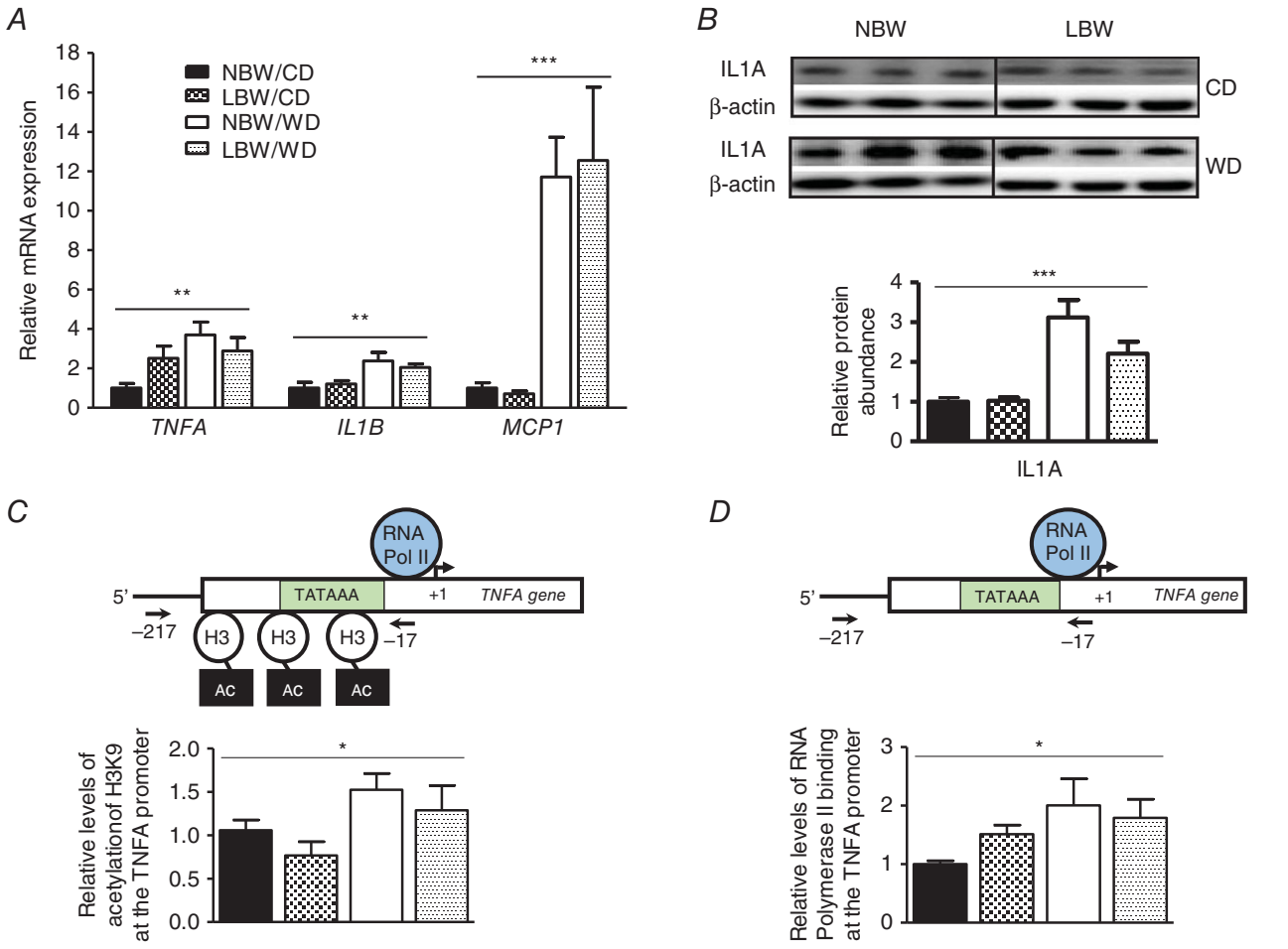

Figure 4. Effect of LBW and WD on hepatic expression of inflammatory markers, levels of acetylated histone H3K9 and RNA polymerase II recruitment at the *TNFA* promoter
A, relative mRNA expression of *TNFA*, *IL1B* and *MCP1*. *B*, IL1A protein abundance and representative Western blots. *C* and *D*, acetylation levels of histone H3K9 and RNA polymerase II recruitment at the *TNFA* promoter region. Data are means ± SEM (n = 4–7 per group). $^{*}P < 0.05$, $^{**}P < 0.01$, $^{***}P < 0.001$ for the main effect of diet independent of birth weight using a two-way ANOVA. NBW/CD *versus* LBW/CD and NBW/WD *versus* LBW/WD were compared using a Bonferroni *post hoc* test. No symbol indicates that there is no statistically significant difference. H3, histone 3; Ac, acetylated; RNA Pol II, RNA polymerase II.

exact mechanisms and the upstream regulators underlying this permanent activation remain to be more thoroughly investigated.

Recently, endogenous, small non-coding RNAs (miRs) have been identified as key epigenetic modulators of liver fibrogenesis. Previous studies have indicated that the expression of miR-146a has been observed to be decreased in liver fibrotic tissues and it has also been suggested as a novel regulator, potentially modulating HSC activation during TGFB1 induction by targeting SMAD4 (He *et al.* 2012*a*). It is intriguing to note in the current study that in young adulthood, we observed a significant decrease in miR-146a expression in conjunction with increased profibrotic SMAD4 protein in LBW offspring, independent of diet. This observation suggests miR-146a as a potential negative regulator of SMAD4 in the liver of LBW offspring. However, whether or not miR-146a or other miRs could modulate HSC activation in LBW offspring is currently unknown. Furthermore, the lack of significant changes in downstream *COL1A1* and *COL3A1* genes, albeit 45% and 260% increases, respectively, over NBW/CD offspring, and the observed minimal fibrosis, do not allow a definitive conclusion with respect to *in utero* induced miRNA effects.

Matrix metalloproteinases (MMPs), a family of ECM degradative enzymes produced by activated HSCs, are regulated by tissue inhibitors of metalloproteinases (TIMPs). MMP production in association with the

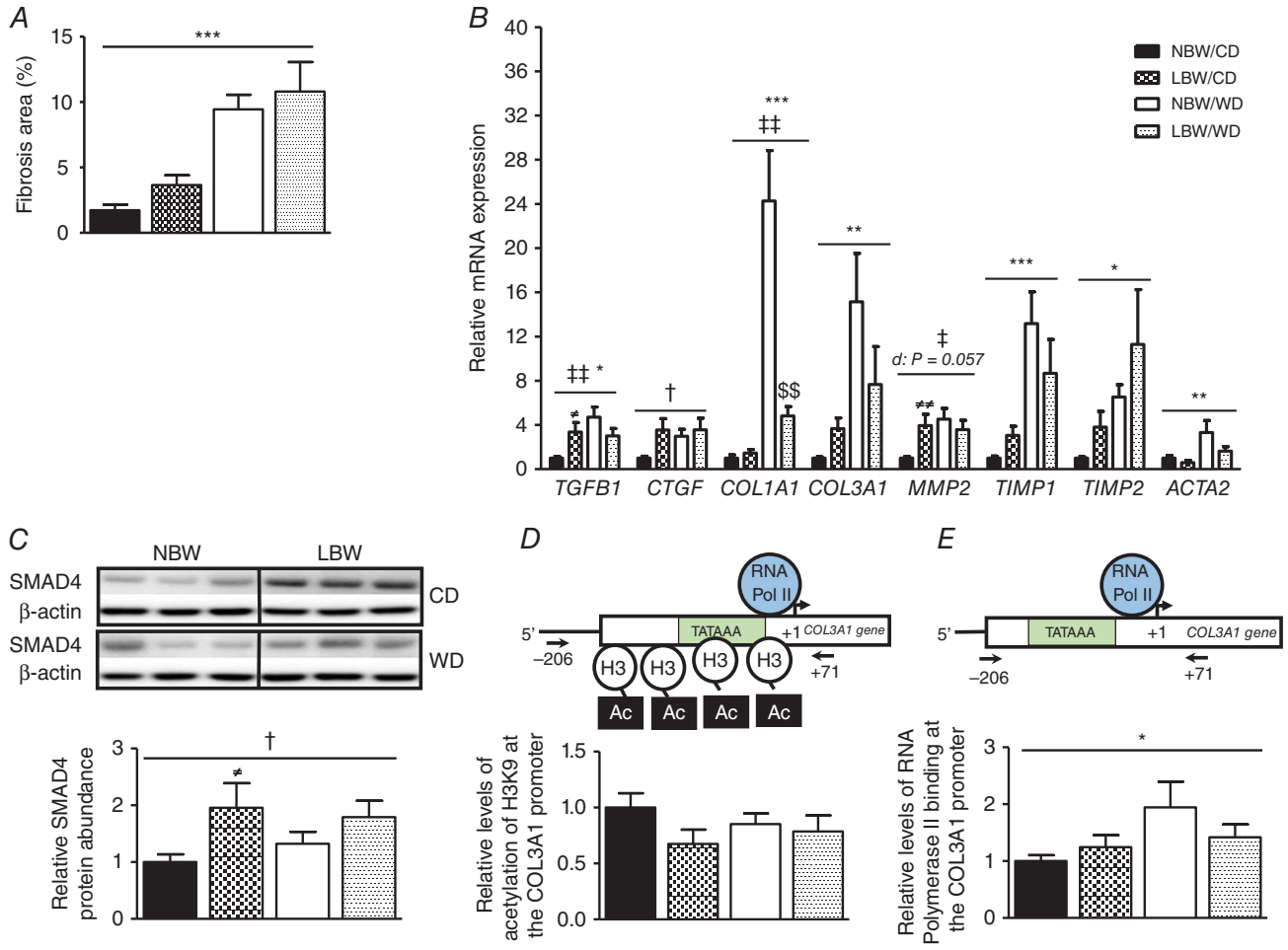

Figure 5. Effect of LBW and WD on the fibrosis area percentage, expression of fibrosis and ECM-related markers, levels of acetylated histone H3K9 and RNA polymerase II recruitment at the *COL3A1* promoter region

A, fibrosis area percentage. *B*, relative mRNA expression of fibrosis and ECM-related genes. *C*, SMAD4 protein level. *D* and *E*, acetylation levels of histone H3K9 and RNA polymerase II recruitment at the *TNFA* promoter region. Data are means ± SEM (n = 5–7 per group). $^{\dagger}P < 0.05$ for the main effect of birth weight; $^{*}P < 0.05$, $^{**}P < 0.01$, $^{***}P < 0.001$ or the indicated P value for the main effect of diet (d); $^{\ddagger}P < 0.05$, $^{\ddagger\ddagger}P < 0.01$ for birth weight and diet interaction (BW × d) using a two-way ANOVA. $^{\neq}P < 0.05$, $^{\neq\neq}P < 0.01$ when comparing NBW/CD *versus* LBW/CD and $^{\$\$}P < 0.01$ when comparing NBW/WD *versus* LBW/WD using a Bonferroni *post hoc* test. No symbol indicates that there is no statistically significant difference. H3, histone 3; Ac, acetylated; RNA Pol II, RNA polymerase II.

increased expression of profibrotic markers such as ACTA2, COL1A1 and COL3A1 is among key process underlying fibrosis development (Lee *et al.* 2001; Mannello & Gazzanelli, 2001; Han, 2006; Ji *et al.* 2012). Previous rodent studies involving the chronic intake of diets enriched in saturated fats, cholesterol and carbohydrates as fructose or sucrose in solid foods or drinking water have also reported an increased expression of ACTA2, a marker of activated HSCs, as well as a mild hepatic periportal fibrosis and increased gene and protein expressions

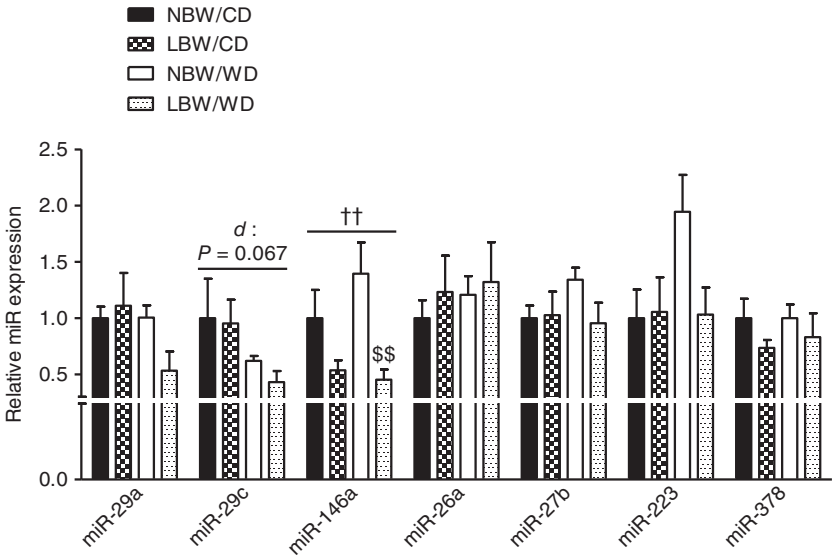

Figure 6. Effect of LBW and WD on hepatic expression of fibrogenesis-related miRs
Expression of miRs was measured by RT-qPCR. Data are means ± SEM (n = 5–7 per group). $^{††}P < 0.01$ represents the main effect of birth weight (BW), the indicated P value designated the main effect of diet (d) using a two-way ANOVA. $^{\$\$}P < 0.01$, when comparing NBW/WD *versus* LBW/WD using a Bonferroni *post hoc* test. No symbol indicates that there is no statistically significant difference.

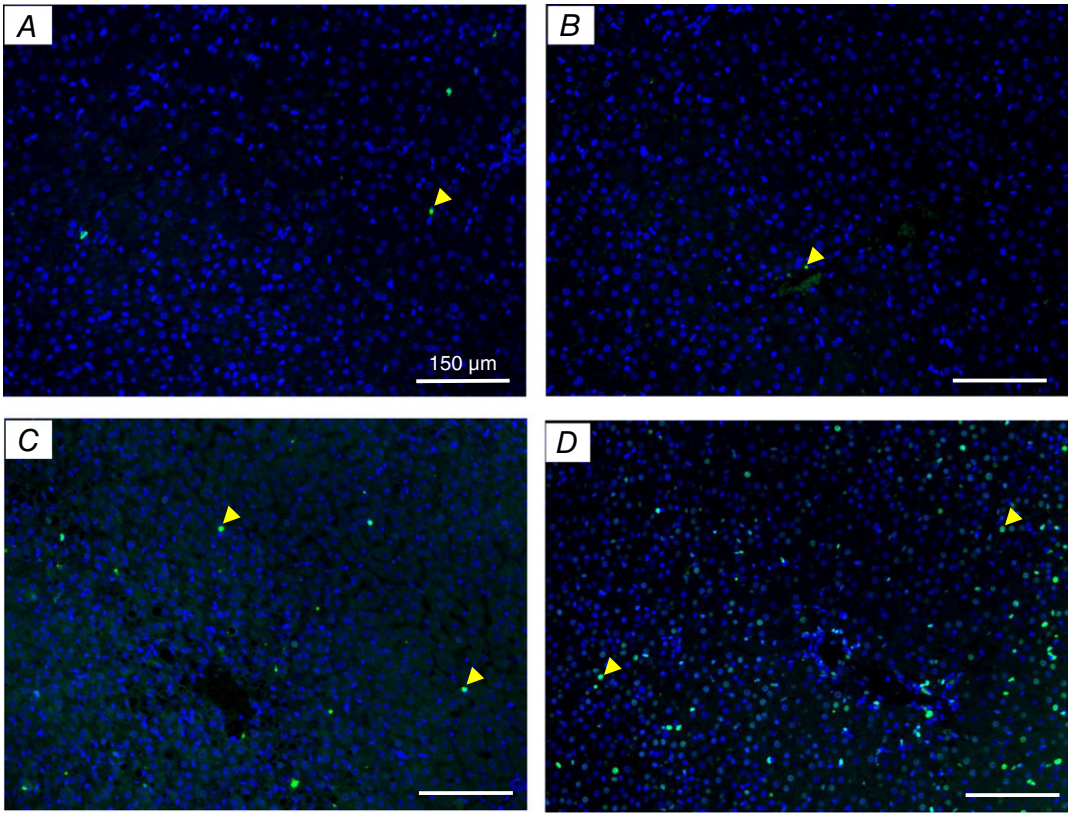

Figure 7. Fluorescent TUNEL staining of liver sections from NBW and LBW offspring fed a CD or WD from weaning to 150 days
Fluorescent TUNEL staining of liver reveals cells positively stained for cell death (indicated by the yellow arrowheads) in NBW/CD (*A*), LBW/CD (*B*), NBW/WD (*C*) and LBW/WD (*D*) offspring. Scale bar = 150 μm.

of fibrotic markers including TGFB1, COL1A1 and TIMP1 (Charlton *et al.* 2011; Panchal *et al.* 2012; Ishimoto *et al.* 2013; Longato, 2013). In the current study, with a relatively high abundance of fats, 46% kcal (∼66% saturated fatty acids by weight), 22% kcal from sucrose and 7.6% kcal from fructose with 0.25% cholesterol (w/w), a mild hepatic perisinusoidal or portal fibrosis and increased *TGFB1, MMP2, COL1A1, COL3A1*, *TIMP1*, *TIMP2* and *ACTA2* mRNA were observed in WD-fed offspring. Therefore, one could speculate that chronic intake of saturated fatty acids in combination with high sugar intake and cholesterol, promotes HSC activation, a profibrogenic pathway, and consequently, hepatic fibrosis. As mono-unsaturated and omega-3, but not omega-6, polyunsaturated fatty acids prevent hepatic fibrosis (Aguilera *et al.* 2005), the elevated ratio of omega-6 to omega -3 fatty acids (15 in WD *versus* 6.6 in CD) could potentially play a role in the latter hepatic fibrosis shown in WD-fed offspring. Moreover,

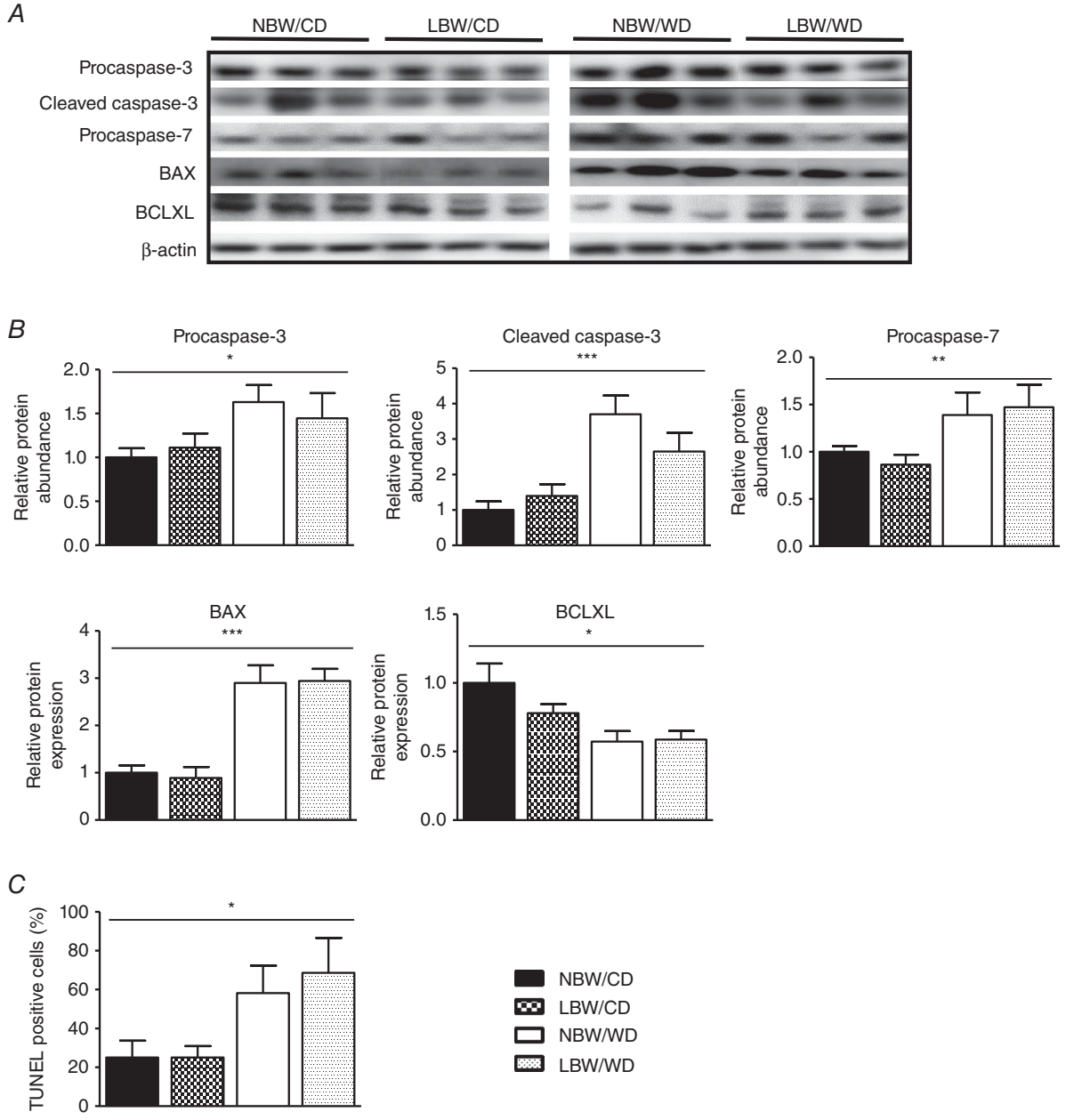

Figure 8. Effect of LBW and WD on apoptosis related proteins and apoptotic cell number
A, representative Western blots. *B*, relative densitometry values of proteins. *C*, quantification of TUNEL positive cells. Data are means ± SEM ($n = 5$–8 per group for Western blots and $n = 4$ per group for the TUNEL assay). $^{*}P < 0.05$, $^{**}P < 0.01$, $^{***}P < 0.001$ for the main effect of diet (*d*) irrespective of birth weight using a two-way ANOVA. NBW/CD *versus* LBW/CD and NBW/WD *versus* LBW/WD were compared using a Bonferroni *post hoc* test. No symbol indicates that there is no statistically significant difference.

the enhanced recruitment of RNA polymerase II at the *COL3A1* promoter in WD-fed offspring, irrespective of birth weight, suggests that life-long intake of a WD leads to transcriptional activation of hepatic fibrosis related genes in young adulthood.

Hepatic triglyceride accumulation, or steatosis, increases the susceptibility of the liver to injury mediated by 'second hits', such as inflammatory cytokines/adipokines, mitochondrial dysfunction and oxidative stress, which in turn lead to steatohepatitis and/or fibrosis (Dowman *et al.* 2010). In the current study, in conjunction with steatosis, proinflammatory factors *TNFA*, *IL1B*, *MCP1* mRNA and IL1A protein were elevated in WD-fed offspring, independent of birth weight. Given that *TNFA* expression is significantly correlated with the degree of fibrosis in NASH patients (Crespo *et al.* 2001), the current WD-induced steatosis and increased expression of proinflammatory markers probably also contribute to fibrosis development in WD-fed offspring. These data thus extend previous studies in mice that have reported hepatic steatosis in association with increased low-grade hepatic inflammation in adult mice fed high fat/high sucrose (for 15 weeks) or high fat/high cholesterol with high fructose in their drinking water (for 25 weeks) (Charlton *et al.* 2011; Ishimoto *et al.* 2013). Considering acetylation of histone H3K9 is known to be a hallmark of chromatin opening (Karmodiya *et al.* 2012), and increased *TNFA* expression in fatty liver of high/fat diet and hyperphagic (ob/ob) mice corresponds to acetylation of histone H3K9 at the *TNFA* promoter (Mikula *et al.* 2014), we also examined whether the *TNFA* expression was epigenetically regulated in WD-fed offspring. Interestingly, in early adulthood we found an increase in acetylated H3K9 associated with an increased RNA polymerase II recruitment at the proximal *TNFA* promoter in liver of WD-fed offspring. Therefore, these findings further demonstrate a chromatin-remodelling-dependent mechanism that potentially contributes to the role of *TNFA* in promoting fibrotic development in WD-fed offspring in early adulthood.

Murine male offspring exposed to prenatal and post-weaning WD (high fat and cholesterol diet) exhibit hepatomegaly characterized by an accumulation of hepatic cholesterol and triglycerides, inflammation and increased expression of *TNFA*, *MCP1* and *TGFB* when compared to offspring exposed to a low fat diet *in utero* followed by a post-weaning WD (Pruis *et al.* 2014). These physiological changes paralleled the presence of advanced steatohepatitis and mirror the current observations in the post-weaning WD situation. Hence, the current study reveals that the high sugar content in the postnatal WD contributes to processes that may mirror the *in utero* programming effect of maternal high fat and cholesterol intake on liver inflammation with concurrent triglyceride accumulation. Moreover, our study expands the observations of murine models, which implicate the

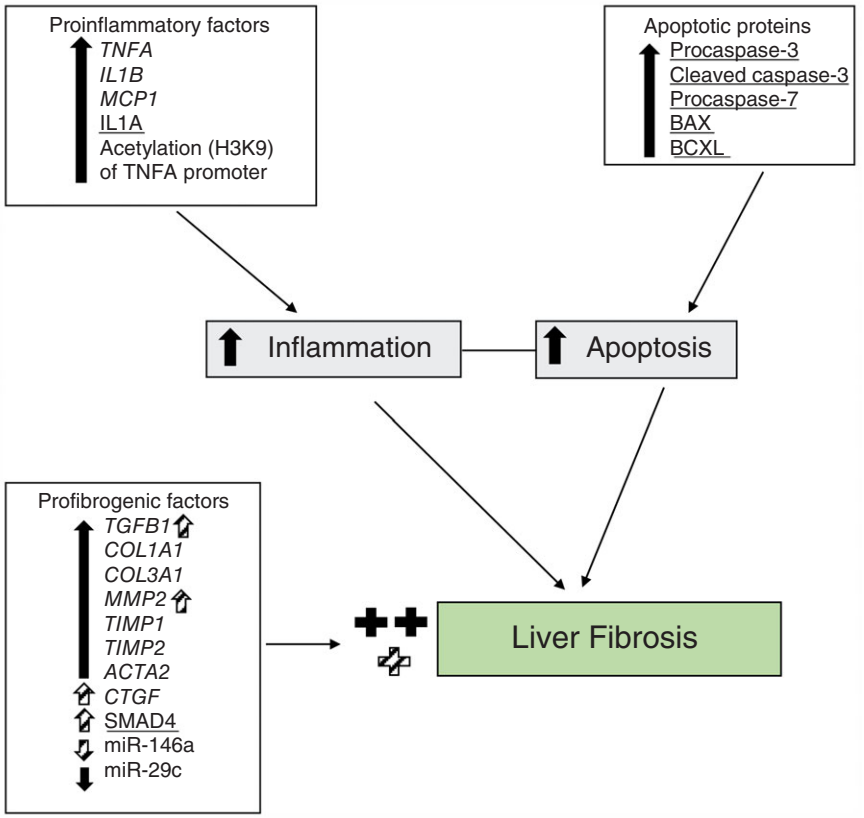

Figure 9. Schematic overview depicting key differentially expressed genes, miRs, proteins and postulated molecular pathways that may be involved in the observed collagen deposition in LBW/CD and in WD-fed (NBW and LBW) guinea pigs
For full explanation and definitions see Abbreviations, Results and Discussion. Arrow shapes designate increased or decreased. Filled arrows and plus shapes indicate changes associated with WD and hatched shapes correspond to modifications related to LBW followed by CD. The two filled plus symbols represent 'mild' and the single hatched plus represents 'minimal'. Genes are italicized and proteins underlined.

harmful effects of adding sugar to a high-fat WD on the liver (Crescenzo *et al.* 2014). Interestingly, body weight in NBW/WD, and LBW/WD offspring especially, tended to be lower than in CD-fed guinea pigs despite a higher calorie intake. As such, these data suggest dysfunctional energy utilization in the WD feeding situation and other studies have reported non-obese outcomes in guinea pig when fed a high fat/high fructose diet (Caillier *et al.* 2012).

Increases in hepatocellular apoptosis frequency is a profibrogenic event in the progression of chronic liver diseases. Indeed, apoptotic bodies and reactive oxygen species stimulate Kupffer cells promoting the release of proinflammatory and profibrogenic cytokines, which induce activation of HSCs (Sanches *et al.* 2015). Yet, the role of pro- and anti-apoptotic proteins in the pathogenesis of WD-induced liver fibrosis is ill defined. Therefore, the induction in procaspase-3, cleaved caspase-3, procaspase-7, the pro-apoptotic BAX protein (Dewson & Kluck, 2009) and the reduced anti-apoptotic factor BCLXL (Janumyan *et al.* 2003) in WD-fed offspring may play a vital role in the pathogenesis of fibrosis in those individuals. This is in support of reports that show imbalances of pro- and anti-apoptotic proteins, in conjunction with an elevated hepatocyte apoptosis activity, play an important role in the pathogenesis of NASH induced by a high/fat diet (Wang *et al.* 2008) and liver fibrosis resulting from consumption of a high fat/high cholesterol diet with high fructose drinking water (Charlton *et al.* 2011). All these observations together suggest an essential role of apoptosis activation in activating liver fibrosis pathways, following chronic unbalanced diet intake as a WD. Importantly, however, LBW alone did not impact apoptosis related proteins, suggesting that the hepatocellular apoptosis pathway may not be a primary mechanism for promoting liver fibrosis in individuals with adverse *in utero* growth.

Conclusion

The present study highlights that an adverse *in utero* environment, one that results in LBW, promotes a specific profibrotic molecular signature in conjunction with minimal fibrosis. Furthermore, the postnatal WD *ad libitum* intake results in steatosis with fibrosis in non-overweight young adult NBW and LBW guinea pigs. The data suggest that the pathways of hepatic fibrosis in the WD offspring involve the combination of saturated fatty acids and sugars resulting in the production of inflammatory and profibrotic cytokines, cell death, collagen deposition and hepatic fibrosis. They also highlight the critical impact of a suboptimal *in utero* environment in modulating hepatic profibrotic genes in early adulthood. Interestingly, at the age studied, there does not appear to be an adverse synergistic effect for LBW combined with WD consumption upon liver fibrosis development. Given the relatively early age of the offspring and the changes in expression of key profibrotic factors in LBW/CD and in WD-fed offspring, a potential trajectory towards a more severe fibrosis with ageing in LBW/WD offspring cannot be excluded.

References

Aguilera CM, Ramirez-Tortosa CL, Quiles JL, Yago MD, Martínez-Burgos MA, Martínez-Victoria E, Gil A & Ramirez-Tortosa MC (2005). Monounsaturated and omega-3 but not omega-6 polyunsaturated fatty acids improve hepatic fibrosis in hypercholesterolemic rabbits. *Nutrition* **21**, 363–371.

Alisi A, Panera N, Agostoni C & Nobili V (2011). Intrauterine growth retardation and nonalcoholic fatty liver disease in children. *Int J Endocrinol* **2011**, 269853.

Andersen AMN & Osler M (2004). Birth dimensions, parental mortality, and mortality in early adult age: A cohort study of Danish men born in 1953. *Int J Epidemiol* **33**, 92–99.

Arai H, Noguchi A, Goto R, Matsuda T, Nakajima H & Takahashi T (2010). Liver fibrosis in an extremely small infant for gestational age. *Tohoku J Exp Med* **221**, 181–185.

Assini JM, Mulvihill EE, Sutherland BG, Telford DE, Sawyez CG, Felder SL, Chhoker S, Edwards JY, Gros R & Huff MW (2013). Naringenin prevents cholesterol-induced systemic inflammation, metabolic dysregulation, and atherosclerosis in $Ldlr^{-}/^{-}$ mice. *J Lipid Res* **54**, 711–724.

Benyon RC & Arthur MJ (2001). Extracellular matrix degradation and the role of hepatic stellate cells. *Semin Liver Dis* **21**, 373–384.

Bhaskar ME (2004). Management of cirrhosis and ascites. *N Engl J Med* **351**, 300–301; author reply 300–301.

Briscoe TA, Rehn AE, Dieni S, Duncan JR, Wlodek ME, Owens JA & Rees SM (2004). Cardiovascular and renal disease in the adolescent guinea pig after chronic placental insufficiency. *Am J Obstet Gynecol* **191**, 847–855.

Caillier B, Pilote S, Patoine D, Levac X, Couture C, Daleau P, Simard C & Drolet B (2012). Metabolic syndrome potentiates the cardiac action potential-prolonging action of drugs: A possible 'anti-proarrhythmic' role for amlodipine. *Pharmacol Res* **65**, 320–327.

Charlton M, Krishnan A, Viker K, Sanderson S, Cazanave SC, McConico A, Masuoko H & Gores GJ (2011). Fast food diet mouse: novel small animal model of NASH with ballooning, progressive fibrosis, and high physiological fidelity to the human condition. *Am J Physiol Gastrointest Liver Physiol* **301**, G825–G834.

Crescenzo R, Bianco F, Coppola P, Mazzoli A, Tussellino M, Carotenuto R, Liverini G & Iossa S (2014). Fructose supplementation worsens the deleterious effects of short-term high-fat feeding on hepatic steatosis and lipid metabolism in adult rats. *Exp Physiol* **99**, 1203–1213.

Crespo J, Cayon A, Fernandez-Gil P, Hernandez-Guerra M, Mayorga M, Dominguez-Diez A, Fernandez-Escalante JC & Pons-Romero F (2001). Gene expression of tumor necrosis factor α and TNF-receptors, p55 and p75, in nonalcoholic steatohepatitis patients. *Hepatology* **34**, 1158–1163.

Dewson G & Kluck RM (2009). Mechanisms by which Bak and Bax permeabilise mitochondria during apoptosis. *J Cell Sci* **122**, 2801–2808.

Dowman JK, Tomlinson JW & Newsome PN (2010). Pathogenesis of non-alcoholic fatty liver disease. *QJM* **103**, 71–83.

Duan X-Y, Pan Q, Yan S-Y, Ding W-J, Fan J-G & Qiao L (2014). High-saturate-fat diet delays initiation of diethylnitrosamine-induced hepatocellular carcinoma. *BMC Gastroenterol* **14**, 195.

Ekstedt M, Franzén LE, Mathiesen UL, Thorelius L, Holmqvist M, Bodemar G & Kechagias S (2006). Long-term follow-up of patients with NAFLD and elevated liver enzymes. *Hepatology* **44**, 865–873.

Fiorentino M, Vasuri F, Ravaioli M, Ridolfi L, Grigioni WF, Pinna AD & D'Errico-Grigioni A (2009). Predictive value of frozen-section analysis in the histological assessment of steatosis before liver transplantation. *Liver Transplant* **15**, 1821–1825.

Folch J, Lees M & Sloane Stanley GH (1957). A simple method for the isolation and purification of total lipides from animal tissues. *J Biol Chem* **226**, 497–509.

Gomez-Pinilla PJ, Gomez MF, Hedlund P, Sward K, Hellstrand P, Camello PJ, Pozo MJ & Andersson KE (2007). Effect of melatonin on age associated changes in guinea pig bladder function. *J Urol* **177**, 1558–1561.

Greulich S, Herzfeld D, Wiza D, Preilowski S, Ding Z, Mueller H, Langin D, Jaquet K, Ouwens DM & Eckel J (2011). Secretory products of guinea pig epicardial fat induce insulin resistance and impair primary adult rat cardiomyocyte function. *J Cell Mol Med* **15**, 2399–2410.

Han YP (2006). Matrix metalloproteinases, the pros and cons, in liver fibrosis. *J Gastroenterol Hepatol* **21**, Suppl. 3, S88–S91.

He Y, Huang C, Sun X, Long XR, Lv XW & Li J (2012*a*). MicroRNA-146a modulates TGF-beta1-induced hepatic stellate cell proliferation by targeting SMAD4. *Cell Signal* **24**, 1923–1930.

He Y, Huang C, Zhang SP, Sun X, Long XR & Li J (2012*b*). The potential of microRNAs in liver fibrosis. *Cell Signal* **24**, 2268–2272.

Hutter D, Kingdom J & Jaeggi E (2010). Causes and mechanisms of intrauterine hypoxia and its impact on the fetal cardiovascular system: a review. *Int J Pediatr* **2010**, 401323.

Iredale JP (2007). Models of liver fibrosis: Exploring the dynamic nature of inflammation and repair in a solid organ. *J Clin Invest* **117**, 539–548.

Ishak K, Baptista A, Bianchi L, Callea F, De Groote J, Gudat F, Denk H, Desmet V, Korb G & MacSween RN (1995). Histological grading and staging of chronic hepatitis. *J Hepatol* **22**, 696–699.

Ishimoto T, Lanaspa MA, Rivard CJ, Roncal-Jimenez CA, Orlicky DJ, Cicerchi C, McMahan RH, Abdelmalek MF, Rosen HR, Jackman MR, MacLean PS, Diggle CP, Asipu A, Inaba S, Kosugi T, Sato W, Maruyama S, Sánchez-Lozada LG, Sautin YY, Hill JO, Bonthron DT & Johnson RJ (2013). High fat and high sucrose (western) diet induce steatohepatitis that is dependent on fructokinase. *Hepatology* **58**, 1632–1643.

Janumyan YM, Sansam CG, Chattopadhyay A, Cheng N, Soucie EL, Penn LZ, Andrews D, Knudson CM & Yang E (2003). Bcl-xL/Bcl-2 coordinately regulates apoptosis, cell cycle arrest and cell cycle entry. *EMBO J* **22**, 5459–5470.

Jeong WI, Do SH, Yun HS, Song BJ, Kim SJ, Kwak WJ, Yoo SE, Park HY & Jeong KS (2004). Hypoxia potentiates transforming growth factor-β expression of hepatocyte during the cirrhotic condition in rat liver. *Liver Int* **24**, 658–668.

Ji J, Yu F, Ji Q, Li Z, Wang K, Zhang J, Lu J, Chen L, Qun E, Zeng Y & Ji Y (2012). Comparative proteomic analysis of rat hepatic stellate cells activation: A comprehensive view and suppressed immune response. *Hepatology* **56**, 332–349.

Karmodiya K, Krebs AR, Oulad-Abdelghani M, Kimura H & Tora L (2012). H3K9 and H3K14 acetylation co-occur at many gene regulatory elements, while H3K14ac marks a subset of inactive inducible promoters in mouse embryonic stem cells. *BMC Genomics* **13**, 424.

Kim J, Lee K, Chang H, Lee W & Lee J (2014). Progression of diet induced nonalcoholic steatohepatitis is accompanied by increased expression of kruppel-like-factor 10 in mice. *J Transl Med* **12**, 186.

Kind KL, Clifton PM, Grant PA, Owens PC, Sohlstrom A, Roberts CT, Robinson JS & Owens JA (2003). Effect of maternal feed restriction during pregnancy on glucose tolerance in the adult guinea pig. *Am J Physiol Regul Integr Comp Physiol* **284**, R140–R152.

Kirillov V, Siler JT, Ramadass M, Ge L, Davis J, Grant G, Nathan SD, Jarai G & Trujillo G (2015). Sustained activation of Toll-like receptor 9 induces an invasive phenotype in lung fibroblasts. *Am J Pathol* **185**, 943–957.

Kleiner DE, Brunt EM, Van Natta M, Behling C, Contos MJ, Cummings OW, Ferrell LD, Liu Y-C, Torbenson MS, Unalp-Arida A, Yeh M, McCullough AJ & Sanyal AJ (2005). Design and validation of a histological scoring system for nonalcoholic fatty liver disease. *Hepatology* **41**, 1313–1321.

Knodell RG, Ishak KG, Black WC, Chen TS, Craig R, Kaplowitz N, Kiernan TW & Wollman J (1981). Formulation and application of a numerical scoring system for assessing histological activity in asymptomatic chronic active hepatitis. *Hepatology* **1**, 431–435.

Kohli R, Kirby M, Xanthakos SA, Softic S, Feldstein AE, Saxena V, Tang PH, Miles L, Miles MV, Balistreri WF, Woods SC & Seeley RJ (2010). High-fructose, medium chain trans fat diet induces liver fibrosis and elevates plasma coenzyme Q9 in a novel murine model of obesity and nonalcoholic steatohepatitis. *Hepatology* **52**, 934–944.

Kwiecinski M, Noetel A, Elfimova N, Trebicka J, Schievenbusch S, Strack I, Molnar L, von Brandenstein M, Töx U, Nischt R, Coutelle O, Dienes HP & Odenthal M (2011). Hepatocyte growth factor (HGF) inhibits collagen I and IV synthesis in hepatic stellate cells by miRNA-29 induction. *PLoS One* **6**, e24568.

Lan HY (2011). Diverse roles of TGF-β/Smads in renal fibrosis and inflammation. *Int J Biol Sci* **7**, 1056–1067.

Lee KS, Lee SJ, Park HJ, Chung JP, Han KH, Chon CY, Lee SI & Moon YM (2001). Oxidative stress effect on the activation of hepatic stellate cells. *Yonsei Med J* **42**, 1–8.

Longato L (2013). Non-alcoholic fatty liver disease (NAFLD): a tale of fat and sugar? *Fibrogenesis Tissue Repair* **6**, 14.

McCullough AJ (2004). The clinical features, diagnosis and natural history of nonalcoholic fatty liver disease. *Clin Liver Dis* **8**, 521–533.

Mannello F & Gazzanelli G (2001). Tissue inhibitors of metalloproteinases and programmed cell death: Conundrums, controversies and potential implications. *Apoptosis* **6**, 479–482.

Matsuzaki K, Murata M, Yoshida K, Sekimoto G, Uemura Y, Sakaida N, Kaibori M, Kamiyama Y, Nishizawa M, Fujisawa J, Okazaki K & Seki T (2007). Chronic inflammation associated with hepatitis C virus infection perturbs hepatic transforming growth factor β signaling, promoting cirrhosis and hepatocellular carcinoma. *Hepatology* **46**, 48–57.

Mehal WZ, Iredale J & Friedman SL (2011). Scraping fibrosis. *Nat Med* **17**, 552–553.

Mikula M, Majewska A, Ledwon JK, Dzwonek A & Ostrowski J (2014). Obesity increases histone H3 lysine 9 and 18 acetylation at Tnfa and Ccl2 genes in mouse liver. *Int J Mol Med* **34**, 1647–1654.

Musso G, Gambino R & Cassader M (2010). Non-alcoholic fatty liver disease from pathogenesis to management: an update. *Obes Rev* **11**, 430–445.

Nagaraja T, Chen L, Balasubramanian A, Groopman JE, Ghoshal K, Jacob ST, Leask A, Brigstock DR, Anand AR & Ganju RK (2012). Activation of the connective tissue growth factor (CTGF)-transforming growth factor β 1 (TGF-β 1) axis in hepatitis C virus-expressing hepatocytes. *PLoS One* **7**, e46526.

Panchal SK, Wong WY, Kauter K, Ward LC & Brown L (2012). Caffeine attenuates metabolic syndrome in diet-induced obese rats. *Nutrition* **28**, 1055–1062.

Pruis MGM, Lendvai A, Bloks VW, Zwier MV, Baller JFW, de Bruin A, Groen AK & Plösch T (2014). Maternal western diet primes non-alcoholic fatty liver disease in adult mouse offspring. *Acta Physiol (Oxf)* **210**, 215–227.

Roderburg C, Urban G-W, Bettermann K, Vucur M, Zimmermann H, Schmidt S, Janssen J, Koppe C, Knolle P, Castoldi M, Tacke F, Trautwein C & Luedde T (2011). Micro-RNA profiling reveals a role for miR-29 in human and murine liver fibrosis. *Hepatology* **53**, 209–218.

Sanches SCL, Ramalho LNZ, Augusto MJ, da Silva DM & Ramalho FS (2015). Nonalcoholic steatohepatitis: A search for factual animal models. *Biomed Res Int* **2015**, 1–13.

Sarr O, Thompson JA, Zhao L, Lee TY & Regnault TRH (2014). Low birth weight male guinea pig offspring display increased visceral adiposity in early adulthood. *PLoS One* **9**, e98433.

Takahara T, Furui K, Funaki J, Nakayama Y, Itoh H, Miyabayashi C, Sato H, Seiki M, Ooshima A & Watanabe A (1995). Increased expression of matrix metalloproteinase-II in experimental liver fibrosis in rats. *Hepatology* **21**, 787–795.

Thompson JA, Gros R, Richardson BS, Piorkowska K & Regnault TRH (2011). Central stiffening in adulthood linked to aberrant aortic remodeling under suboptimal intrauterine conditions. *Am J Physiol Regul Integr Comp Physiol* **301**, R1731–R1737.

Thompson JA, Sarr O, Piorkowska K, Gros R & Regnault TRH (2014). Low birth weight followed by postnatal over-nutrition in the guinea pig exposes a predominant player in the development of vascular dysfunction. *J Physiol* **592**, 5429–5443.

Turner AJ & Trudinger BJ (2009). A modification of the uterine artery restriction technique in the guinea pig fetus produces asymmetrical ultrasound growth. *Placenta* **30**, 236–240.

Wang Y, Ausman LM, Russell RM, Greenberg AS & Wang X-D (2008). Increased apoptosis in high-fat diet-induced nonalcoholic steatohepatitis in rats is associated with c-Jun NH_2-terminal kinase activation and elevated proapoptotic Bax. *J Nutr* **138**, 1866–1871.

Wang Y, Huang Y, Guan F, Xiao Y, Deng J, Chen H, Chen X, Li J, Huang H & Shi C (2013). Hypoxia-inducible factor-1alpha and MAPK co-regulate activation of hepatic stellate cells upon hypoxia stimulation. *PLoS One* **8**, e74051.

Yang C, Zeisberg M, Mosterman B, Sudhakar A, Yerramalla U, Holthaus K, Xu L, Eng F, Afdhal N & Kalluri R (2003). Liver fibrosis: Insights into migration of hepatic stellate cells in response to extracellular matrix and growth factors. *Gastroenterology* **124**, 147–159.

Additional information

Competing interests

None declared.

Author contributions

The experiments were performed at The Susan Vitali-Lovell Laboratory for Studies in Fetal Programming of Human Health Risks (Western University, London, ON, Canada). O.S. and T.R.H.R. conceived and designed the research; O.S., A.B., J.A.T., L.Z., K.R. and T.R.H.R. conducted the research; O.S., T.R.H.R., I.W. and J.C.W. analysed the data; and O.S. and T.R.H.R. wrote the paper. A.B., J.A.T., L.Z., K.R., I.W. and J.C.W. critically reviewed the paper. T.R.H.R. had primary responsibility for the final content. All authors have approved the final version of the manuscript and agree to be accountable for all aspects of the work. All persons designated as authors qualify for authorship, and all those who qualify for authorship are listed.

Funding

This work was supported by the Canadian Institutes of Health Research (Operating Grant No. MOP-209113). O. Sarr was supported by a Whaley Postdoctoral Fellowship.

Acknowledgements

The authors thank Brad Matushewski for his assistance with animal surgeries and Cynthia G. Sawyez for biochemical measurements.

Translational perspective

The effects of placental insufficiency-induced low birth weight followed by a post-weaning Western diet (WD) on excessive collagen deposition within the liver (hepatic fibrosis) were evaluated with the use of a guinea pig model of low birth weight (LBW) and postnatal WD feeding. Analyses included changes in inflammation and apoptosis pathways in association with fibrogenesis in offspring born small due to placental insufficiency and offspring born with a normal body weight, both fed either a post-weaning control diet or WD high in saturated fat, sugars and cholesterol. Our findings show that young adult offspring born LBW, even fed a normal post-weaning diet, display hepatic activation of fibrotic genes and minimal liver fibrosis when compared to normal birth weight offspring fed the same diet. Interestingly, both offspring born LBW or normal birth weight, when fed WD, exhibit a significant fatty liver, hepatic inflammation, liver cell death and mild fibrosis in early adulthood. Independently of birth weight, WD also altered the expression of genes and proteins that regulate hepatic inflammation, liver cell death and fibrosis. However, these changes were not exacerbated in offspring born LBW and fed the post-weaning WD when compared to offspring born with a normal body weight and fed the post-weaning WD. Together, these data highlight the individual importance of the intrauterine environment and postnatal nutrition in long-term liver health. This study supports the relevancy of the guinea pig model in future *in vivo* studies, particularly targeting fibrotic liver disease subsequent to adverse pre- and postnatal environments, in non-overweight individuals.